Effect of Structural Order on the Dark Current and Photocurrent in Zinc Octakis(β-decoxyethyl)porphyrin Thin-Layer Cells

Chong-Yang Liu, Horng-Long Pan, Huajun Tang, Marye Anne Fox,* and Allen J. Bard*

Department of Chemistry and Biochemistry, The University of Texas at Austin, Austin, Texas 78712

Received: July 30, 1994; In Final Form: October 4, 1994[⊗]

The conductivity (dark and photo) and the short-circuit photocurrent in symmetrical thin-layer cells containing zinc octakis(β-decoxyethyl)porphyrin (ZnODEP) were determined as functions of temperature with the ZnODEP in the solid, liquid crystal, and isotropic liquid states. ZnODEP, a discotic liquid crystal, organizes to form columns, which act as one-dimensional conductors, in the solid and liquid crystal phases. The changes in conductivity and photocurrent are interpreted by changes in structure and disordering (melting) that affect the rate of charge transport and trapping in the ZnODEP layer.

Introduction

We describe measurements of dark conductivity, photoconductivity, and photocurrent in a cell containing a thin film of zinc octakis(β-decoxyethyl)porphyrin (ZnODEP)[1] as functions of temperature to probe charge transport in the quasi-one-dimensional photoconductor. These measurements allow us to propose a correlation between structural order and charge carrier transport within ZnODEP. With increasing temperature, the crystal changes from a well-ordered solid structure into a liquid crystal (at 95 °C) and then into a nonordered isotropic liquid (at 147 °C). The photocurrent and dark current show a parallel response as a function of temperature to the changes in the ZnODEP structure. Such studies are useful in the characterization of organic molecular crystals, which have been proposed recently for applications in areas such as electronics, optics, and reprographics.[2−4] Moreover, a knowledge of temperature effects is important for the operation of devices based on ZnODEP.[1]

The chemical structure of the ZnODEP molecule is characterized by a flat aromatic core surrounded by eight hydrocarbon chains (Figure 1A). The distances shown in this figure are taken from previous studies on conventional metalloporphyrins[5] and hydrocarbon chains[6] and assume that the paraffinic tails are fully elongated. In the crystal, the molecules are regularly stacked to form individual columns (Figure 1B). The molecule-to-molecule separation within the same column is about 3.98 Å, and the intercolumn distance is 23.59 Å, as determined by X-ray diffraction studies described elsewhere.[7] This structure suggests that the solid film is an anisotropic (one-dimensional) electronic conductor in which conduction takes place along the individual columns, where there is good intermolecular $\pi-\pi$ overlap, in a direction perpendicular to the molecular plane. Since the porphyrin rings are spaced by more than 15 Å apart by the nonpolar hydrocarbon chains, each molecular column formed by the aromatic cores behaves as a "molecular wire"; the assembly of such stacks constitutes the molecular crystal. Traps for charge carriers would be created by structural imperfections, such as dislocations, vacancies, and point defects. In fact, high-density data storage based on charge trapping within ZnODEP has been demonstrated.[1]

Because organic molecular crystals are held together by weak intermolecular van der Waals interaction forces, they are very different than inorganic covalent or ionic crystals in their

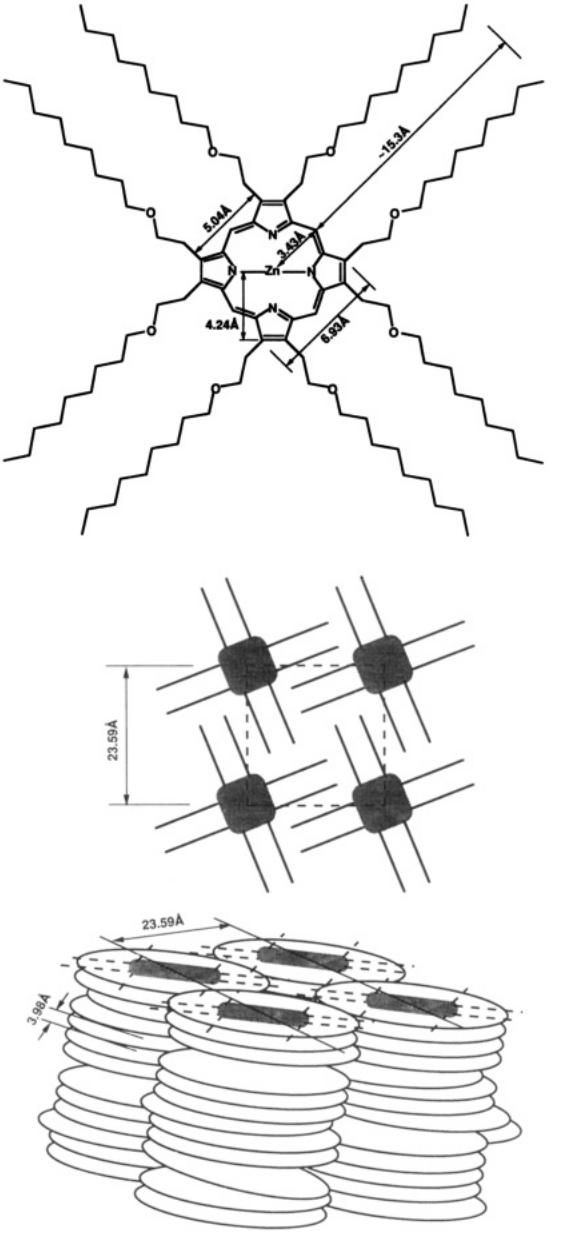

Figure 1. (A, top) Chemical structure of the zinc octakis(β-decoxyethyl)porphyrin (ZnODEP) molecule. (B, bottom) Schematic diagram of the crystal structure of ZnODEP: upper, top view; lower, side view with crystal defects.

[⊗] Abstract published in *Advance ACS Abstracts,* May 1, 1995.

0022-3654/95/2099-7632$09.00/0

mechanical, optical, and electronic properties.[8-10] For example, the primary process for charge transport within the molecular crystals is hopping by tunneling or resonance transfer.[8,9] Charge carriers are localized within individual molecules, so that the estimated mean free path of the charge carrier is often much smaller than the elementary cell parameter.[8] This implies that charge carriers are scattered on molecules of the lattice, so that charge trapping and hopping within the ZnODEP films should be very sensitive to the structural order of the molecular crystal. To test this concept, we undertook a systematic study of the temperature dependence of photocurrent and dark current with ZnODEP sandwich cells (i.e., ITO/ZnODEP/ITO).[1,11]

Experimental Section

MODEP (M = Zn, Co, Cu, and Pd) was synthesized and purified by the method of Gregg et al.[11] The general procedures for the fabrication of ITO/ZnODEP/ITO symmetrical cells used here have been described previously.[1,11] Briefly, two pieces of ITO-coated glass on which ITO was removed on three edges by chemical etching in sulfuric acid were brought together to form an empty cell separated by ca. 1−2 μm epoxy spacers. These spacers only contacted the glass substrates and were therefore out of the circuit and eliminated possible leakage of current, especially at high temperatures. ZnODEP powder was placed at the cell opening and was capillary-filled into the cell by heating to slightly above its melting point (~147 °C) in air. The cell was then cooled slowly to room temperature. Oxygen appeared unimportant to the cell performance, as reported earlier.[11] Optical absorption spectra of the thin-layer cells were measured on a Hewlett-Packard 8451A single-beam spectrophotometer. The spectra were essentially identical to that of ZnOOEP,[11] since the length of the alkyl chains has no effect on the photophysics.[11]

For X-ray diffraction analysis, films of ZnODEP on an ITO substrate were prepared from a symmetrical sandwich cell in which the top layer of ITO was removed after capillary filling had been completed. Thicker films (~10 μm) were used to reduce the background level of ITO. X-ray data were collected by the scan method from low to high angle using a Philips diffractometer (PW 1710) and a Philips X-ray generator (PW 1729). Signals were recorded on a Philips one-line recorder (PW 700). The voltage of the power generator and the current of the X-ray tube were 40 kV and 40 mA, respectively.

For the temperature-dependent current measurements, the cell was placed inside a thick (~1.5 cm) copper box which has a high thermal capacity to keep the temperature uniform and to minimize the temperature fluctuation. The box was then placed in an oven and located about 10 cm away from each wall. The temperature was controlled with an Omega CN76000 temperature programmer. Current−temperature measurements were carried out with a Princeton Applied Research 175 universal programmer, a Model 173 potentiostat, and a home-built high-sensitivity current amplifier. The signal was recorded on a Kipp & Zonen $x-yy$ recorder. A fiber-optic illuminator was used as the light source which irradiated the sample through glass windows in the oven and the copper box at an intensity of ca. 10 mW/cm^2.

Phase transitions of the liquid crystal ZnODEP were characterized by differential scanning calorimetry (DSC) on either a Perkin-Elmer TG-7 or a Mettler FP 80184 instrument. The DSC cells were independent dual furnaces constructed of a platinum−iridium alloy with independent platinum resistance heaters and temperature sensors. The calorimeters were calibrated against high-purity indium as a standard. The calorimetric and temperature accuracy were ±1% and ±1 °C, respectively.

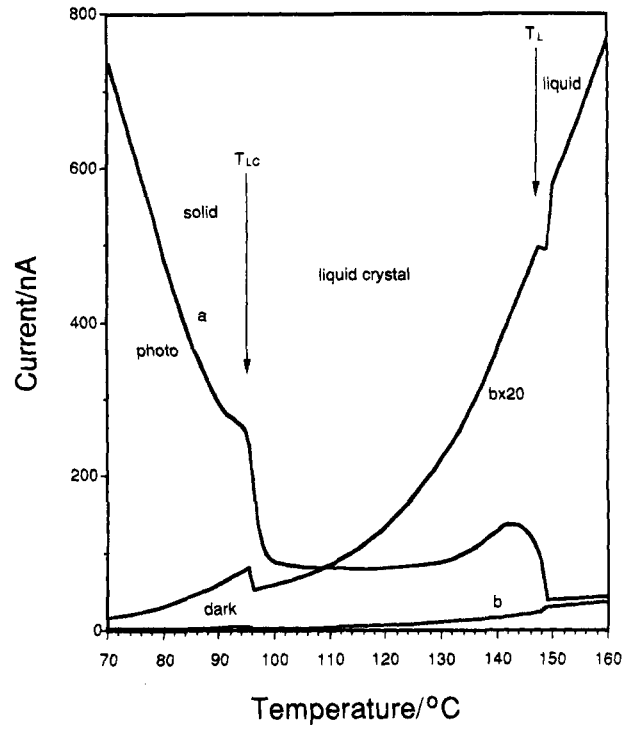

Figure 2. Steady-state photocurrent (curve a) and dark current (curve b) as functions of temperature. Curve b×20 is dark current enlarged 20 times. Heating rate, 2 °C/min; bias potential, 250 mV; light intensity, 10 mW/cm^2; film thickness, 1.5 μm; cell area, 0.3 cm^2.

Results and Discussion

As shown in Figure 2, the steady-state photocurrent under a bias of 250 mV decreased with a temperature increase and dropped sharply at the temperature where the solid to liquid crystal phase transition (T_{LC}) occurred (curve a). In the liquid crystal region, the photocurrent remained fairly constant over a temperature range of 30 °C, then gradually increased with a further increase in temperature, and finally decreased abruptly at the temperature where the liquid crystal to isotropic liquid phase transition (T_L) occurred. Interestingly, a very small photocurrent was still seen in the disordered isotropic liquid phase of ZnODEP. In contrast, as shown in Figure 2 (curve b), the dark current increased with temperature and decreased slightly at T_{LC}, as shown more clearly in the enlarged curve (curve b×20). This dark current increased throughout the whole liquid crystal mesophase and, after a slight drop, increased sharply at T_L. The dark current continuously increased in the isotropic liquid phase. Curve a in Figure 2 was obtained under irradiation and contains contributions from both photocurrent and dark currents, although the latter are too small to make any appreciable contribution to the major features at the two phase transitions. During the experiment, the background level (dark current) was checked every 10 °C by shutting off the irradiation for a few seconds. The background level at the check points fell on curve b in Figure 2. These results were reproducible on sequential temperature cycles. When the sign of the bias applied to the sandwich cell was changed from positive to negative, the current direction simply reversed without significant changes in the curves.

An increase in temperature can cause a number of effects. Thermal excitation of charge carriers from traps created by structural disorders or chemical impurities can increase the population of charge carriers for electric conduction. We believe

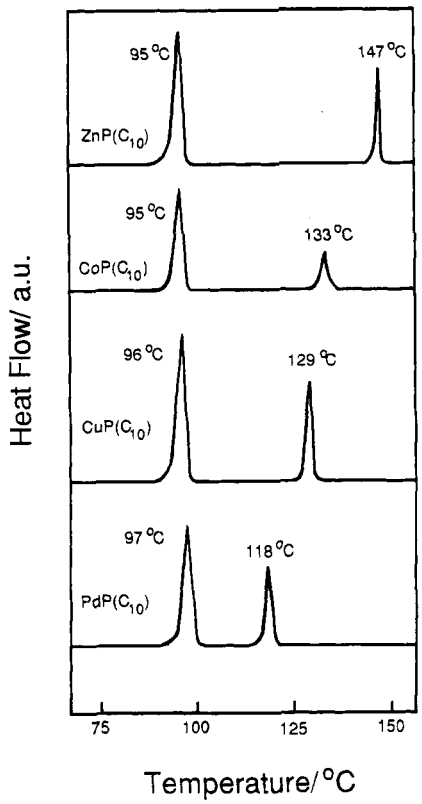

Figure 3. Differential scanning calorimogram of MODEP (M = Zn, Co, Cu, and Pd). Heating rate 10 °C/min.

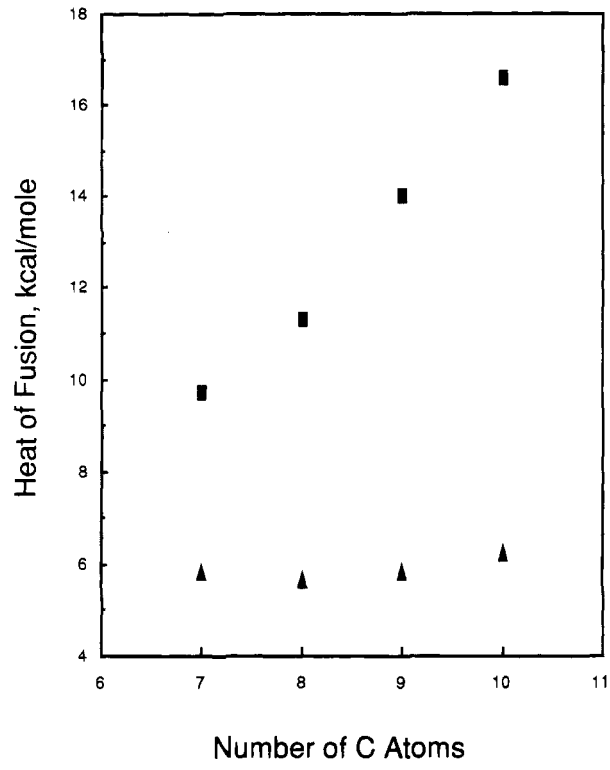

Figure 4. Dependence of the heat of fusion on the number of carbon atoms for the alkyl chains at the phase transitions on going from solid state to mesophase (■) and from mesophase to isotropic liquid (▲).

this is the major contribution to the dark current increase. An increase in temperature can also lead to an increase in the mobility of ionic impurities. Thermal excitation is a much smaller effect than optical excitation in increasing the charge carrier population and, therefore, probably plays a negligible role in the photocurrent behavior. This is clearly seen by a comparison of the magnitude of the dark current to the photocurrent. Under illumination, both scattering events and charge trapping and detrapping processes are enhanced by a temperature increase, and these lead to a decrease in charge carrier mobility.[12-15] As a result, recombination of electron–hole pairs generated by the irradiation will increase and give rise to a photocurrent decrease. Indeed, a mobility decrease with T was observed with the time-resolved microwave conductivity technique.[16]

At T_{LC}, the ZnODEP molecular crystal is partially melted, that is, the long hydrocarbon chains become more flexible. This conclusion is supported by a number of experimental results. (1) The heat of fusion was much larger at T_{LC} than at T_L, as shown in Figure 3. This observation is consistent with the greater mass of the MODEP (M = Zn, Cu, Co, and Pd) molecules in the side chains relative to the aromatic rigid core. (2) T_L of MODEP strongly depends on the identity of the metal center in the aromatic core, while T_{LC} showed essentially no sensitivity to the metal center, within 2 °C (Figure 3). (3) With increasing length of the alkyl tails, the heat of fusion increased significantly at T_{LC}, but remained almost constant at T_L within experimental error, as shown in Figure 4. (4) X-ray diffraction data proved that the column structure still remained in the liquid crystal mesophase,[7] and crystalline domains were clearly seen between two-crossed polarizers.[17] The main contribution to the heat of fusion from crystal to mesophase is therefore attributed to the melting of the long hydrocarbon chains. The same conclusion was drawn from the studies of related phthalocyanine-based liquid crystals also with paraffinic chains.[18]

The transition at T_{LC}, where the long tails change from rigid to flexible, causes a drop in photoconductivity. Given the one-dimensional nature of the conductivity, this drop may represent fluctuations in the spacings between molecules or increased lateral movements of the molecules within the same column. This will perturb charge carrier hopping and, hence, carrier mobility along a column. The same effect can be seen in the enlarged dark current curve (Figure 2). However, both currents did not disappear completely after the first phase transition, since molecular columns, and thus electrical conduction, still exist in the liquid crystalline state.

The scattering processes which limit charge carrier mobility seem to saturate at the mesophase stage, as evidenced by a fairly constant photocurrent. However, the thermal detrapping process increased with temperature, leading to continuously increasing dark current over the whole liquid crystalline range. A thermal excitation-induced population increase produces the opposite trend in electrical conduction with temperature as compared to the scattering events. Since optical excitation dominates charge carrier generation, the photocurrent (Figure 2, curve a) mainly reflects mobility changes with temperature. On the other hand, the dark current is controlled by both mechanisms. Since the scattering appears to saturate in the mesophase, the dark current increased more quickly with temperature in the liquid crystalline state compared to the solid state.

Another important mechanism which could influence the charge carrier mobility is scattering by ionized impurities.[13-15] Thermal detrapping and ionization of chemical impurities should cause two effects. They increase the charge carrier population, which is favorable to electrical conduction, especially in the dark current as discussed above. However, they also increase the ionized impurity density, which can lead to trapping and a reduction in the mobility of charge carriers and, therefore, to a lowering of the photocurrent and dark current. This could provide an additional explanation as to why the dark current increased more slowly and the photocurrent decreased more

quickly in the solid phase relative to the liquid crystalline state. At higher temperatures, the photoconductivity of the mesophase shows an increase with increasing temperature. A similar effect is seen in the ionizing radiation-induced conductivity of this material as measured by a microwave technique.[16] An explanation of this effect can be proposed, in analogy to inorganic semiconductors, where scattering of charge carriers from ionized impurities decreases with an increase in temperature.[13-15]

At T_L, where the ordered molecular columns collapse into a completely disordered isotropic liquid, the photocurrent shows another sharp drop. Beyond T_L, both the photocurrent and dark current curves (a and b) almost coincide. As with the photocurrent, the dark current showed an initial small drop at T_L, where columns become disrupted, and then increased.

Charge generation by irradiation does not appear to contribute significantly in the liquid phase, probably because of rapid electron−hole recombination. Moreover, dark charge injection to ZnODEP at the ITO interfaces cannot take place at the small applied bias. Thus, charge hopping between ZnODEP centers or migration of charged ZnODEP species does not contribute to the conductivity. However, impurities that were held in the lattice at lower temperatures become mobile in the liquid phase. These might undergo electron-transfer reactions at the ITO electrodes or, if ionic, contribute directly to the dark conductivity. The shift of governing role in electronic transport from charge hopping in the well-ordered molecular crystal to impurity migration in the structurally disordered liquid gives rise to the sharp increase in the dark current, but a decrease in the photocurrent at T_L, as shown in Figure 2. In the liquid state, the dark current continuously increased with temperature. The photocurrent, however, was essentially constant to 180 °C.

Symmetrical ZnODEP cells are capable of producing considerable steady-state short-circuit photocurrents, as reported earlier.[11] In this case, interfacial charge separation at the irradiated surface provides the driving force for the generation of photocurrent. Weak irradiation (~10 mW/cm^2) was employed to study the dependence of the current vs temperature curves on the bias potential applied to the sandwich cells. New features developed at both phase transitions when the external bias became smaller, as shown in Figure 5. Curve a in this figure was obtained at a bias of +20 mV, and curve b was obtained without bias. Two spikes are seen at T_{LC} and T_L under short-circuit conditions. A change of the shoulders in Figure 2, curve a, to the spikes in Figure 5, curve b, was also observed when a negative bias was applied initially. Interestingly, a larger current spike was seen in the I vs. T curve when the temperature decreased from the disordered liquid phase to the ordered liquid crystal phase under no bias (Figure 5, curve c). While the I vs T curves at a given bias for a temperature increase and decrease (i.e., forward and reverse scans) were very similar, at short circuit the spikes were in opposite directions at T_{LC} and a much larger spike was seen at T_L (Figure 5, curve c). We propose that the photocurrent spikes seen in the heating and cooling curves are caused by charge trapping and detrapping processes. Charge trapping within the ZnODEP film is an important characteristic of the molecular crystal, as reported previously.[1] At the first phase transition from the solid to the liquid crystal phase, the long hydrocarbon chains change from rigid to flexible, as discussed above, and the aromatic central core becomes more mobile. As in an annealing process, molecules around defect sites can gain enough thermal energy to reorder. Thus, defect-induced trapping sites can release charges stored in the solid phase and give rise to a discharge current spike (Figure 5, curve b). The image spike shown in curve c of Figure 5 at the same

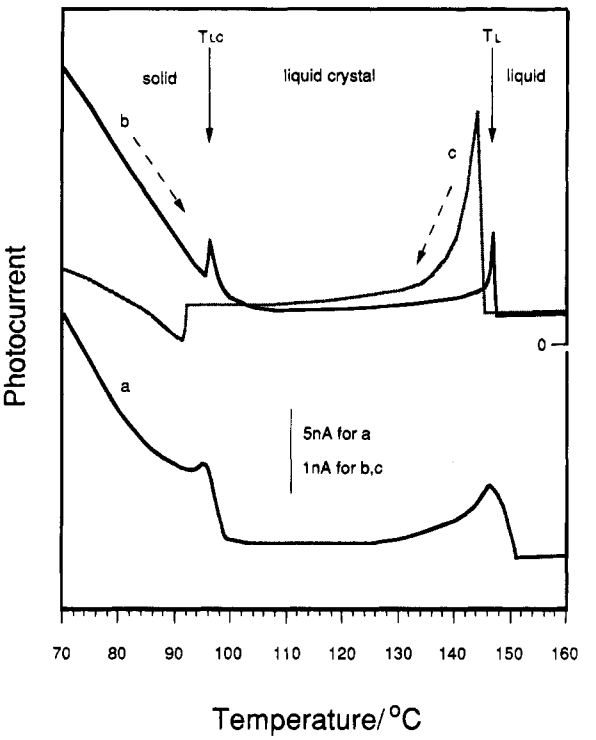

Figure 5. Steady-state photocurrent as a function of temperature: curve a, under a bias of 20 mV; curve b, at short circuit on heating to the liquid state; curve c, at short circuit on cooling to the solid state. Heating rate, 2 °C/ min; light intensity, 10 mW/cm^2; film thickness, 1.5 μm; cell area, 0.3 cm^2.

phase transition may reflect the opposite process, that is, a freezing of defects which induces charge trapping.

At the second phase transition, T_L, the ordered structure of the liquid crystal breaks down, and residual impurities which were embedded within the crystal at mesophase are liberated as the molecular columns melt. Thus, trapping sites related to chemical impurities, at least near the electrode surface, are able to release charges and become ionized. Consequently, a discharge spike is seen (Figure 5, curve b). The nature of the impurities, however, is not clear at present. Ideally, measurements with an ultrapure sample which has been doped with specific ionic impurities could probe this effect. This approach has been widely used for inorganic materials such as Si but is less feasible with organic materials, mainly because of difficulties in purifying them.

Note that a small short-circuit photocurrent is observed above T_L. In the liquid phase, the ITO/ZnODEP/ITO sandwich structure is similar to a thin-layer electrochemical cell. Upon irradiation, electrons could be injected from the excited states of ZnODEP molecules near the interface into the ITO electrode, just as in the solid state. However, the mobility of photogenerated holes to the counter electrode is decreased in the liquid molecular layer, because of a decrease in the order of the crystal structure, and a double-layer structure is created under irradiation at the interface; negative charges accumulate in the ITO electrode and positive charges at the liquid surface layer, with the latter distributed in a diffuse layer.[19] Although recombination takes place at the interface during irradiation, a steady-state double layer exists because the differential charge transfer at the interface is maintained in the liquid state. As the temperature decreases, the randomly oriented ZnODEP molecules in the liquid state reorder into a regular molecular crystal at the transition to mesophase. When this happened during cooling, at the melting point, electrically conducting channels, i.e., the molecular columns, formed between the two electrodes,

and the interfacial double-layer accumulations discharged through these freshly formed molecular wires. Indeed, this process was experimentally observed as a discharge spike shown in curve c in Figure 5 at the clearing point. A further decrease in temperature led to reduction of charge carrier mobility throughout the entire mesophase, which is the reverse process described above. In the solid phase, the photocurrent increased with decreasing temperature and eventually reached the starting point at room temperature (~25 °C) after a slow recovery.

Conclusions

Charge carrier hopping, trapping, and scattering within one-dimensional molecular columns of ZnODEP have been probed by photocurrent and dark current measurements. A clear relationship between crystal structural order and current was obtained from changes at phase transition points. Self-ordering and self-healing were found at T_{LC} where defect-induced charge trapping and detrapping were indicated by photocurrent spikes. Large changes take place when the conducting molecular columns collapse into a disordered isotropic liquid.

Acknowledgment. We are indebted to Dr. F.-R. F. Fan for valuable discussions. The support of this work by the Texas Advanced Research Program and Texas Instruments is gratefully acknowledged.

References and Notes

(1) Liu, C.-Y.; Pan, H.-L.; Fox, M. A.; Bard, A. J. *Science* **1993**, *261*, 897.

(2) Gregory, P. *High-Technology Applications of Organic Colorants*; Plenum Press: New York, 1991.

(3) Simon, J. In *Nanostructures Based on Molecular Materials*; Göpel, W., Ziegler, Ch., Eds.; VCH: Weinheim, 1992; p 267.

(4) Marks, T. J. *Science* **1985**, *227*, 881 and references therein.

(5) Fleischer, E. B. *Acc. Chem. Res.* **1970**, *3*, 105.

(6) *Polymer Handbook*; Brandrup, J., Immergut, E. H., Eds.; John Wiley & Sons: New York, 1975.

(7) Calculated from data in: Pan, H.-L. Ph.D. Dissertation, University of Texas at Austin, 1992.

(8) Silinsh, E. A. *Organic Molecular Crystals, Their Electronic States*; Springer-Verlag: Berlin, 1980.

(9) Simon, J.; André, J.-J. *Molecular Semiconductors: Photoelectrical Properties and Solar Cells*; Springer-Verlag: Berlin, 1985.

(10) Wright, J. *Molecular Crystals*; Cambridge University Press: Cambridge, 1987.

(11) Gregg, B. A.; Fox, M. A.; Bard, A. J. *J. Phys. Chem.* **1990**, *94*, 1586; *J. Phys. Chem.* **1989**, *93*, 4227.

(12) Pankove, J. I. *Optical Processes in Semiconductors*; Dover: New York, 1975.

(13) Wang, S. *Fundamentals of Semiconductor Theory and Device Physics*; Prentice-Hall: Englewood Cliffs, NJ, 1989.

(14) Sze, S. M. *Physics of Semiconductor Devices*, 2nd ed.; John Wiley & Sons: New York, 1981.

(15) Seeger, K. *Semiconductor Physics*; Springer-Verlag: New York, 1973.

(16) Schouten, P. G.; Warman, J. M., de Haas, M. P.; Fox, M. A.; Pan, H.-L. *Nature* **1991**, *353*, 736.

(17) Gregg, B. A.; Fox, M. A.; Bard, A. J. *J. Am. Chem. Soc.* **1989**, *111*, 3024.

(18) Simon, J.; Bassoul, P. In *Phthalocyanines, Properties and Applications*; Leznoff, C. C., Lever, A. B. P., Eds.; VCH: New York, 1989; Vol. 2, p 223.

(19) Bard, A. J.; Faulkner, L. R. *Electrochemical Methods: Fundamentals and Applications*; John Wiley & Sons: New York, 1980.

JP9419860